

This article was downloaded by:

On: 26 January 2011

Access details: *Access Details: Free Access*

Publisher *Taylor & Francis*

Informa Ltd Registered in England and Wales Registered Number: 1072954 Registered office: Mortimer House, 37-41 Mortimer Street, London W1T 3JH, UK



## Liquid Crystals

Publication details, including instructions for authors and subscription information:

<http://www.informaworld.com/smpp/title~content=t713926090>

### The molecular and crystal structure of 4-methoxybenzylidene-4'-*n*-butylaniline (MBBA) at -163°C

R. Boese<sup>a</sup>; M. Yu. Antipin<sup>ab</sup>; M. Nussbaumer<sup>a</sup>; D. Bläser<sup>a</sup>

<sup>a</sup> Institut für Anorganische Chemie der Universität-GH Essen, Essen 1, Germany <sup>b</sup> Institute of Organoelement Compounds, Russian Academy of Sciences, Moscow, Russia

**To cite this Article** Boese, R. , Antipin, M. Yu. , Nussbaumer, M. and Bläser, D.(1992) 'The molecular and crystal structure of 4-methoxybenzylidene-4'-*n*-butylaniline (MBBA) at -163°C', *Liquid Crystals*, 12: 3, 431 – 440

**To link to this Article:** DOI: 10.1080/02678299208031059

**URL:** <http://dx.doi.org/10.1080/02678299208031059>

PLEASE SCROLL DOWN FOR ARTICLE

Full terms and conditions of use: <http://www.informaworld.com/terms-and-conditions-of-access.pdf>

This article may be used for research, teaching and private study purposes. Any substantial or systematic reproduction, re-distribution, re-selling, loan or sub-licensing, systematic supply or distribution in any form to anyone is expressly forbidden.

The publisher does not give any warranty express or implied or make any representation that the contents will be complete or accurate or up to date. The accuracy of any instructions, formulae and drug doses should be independently verified with primary sources. The publisher shall not be liable for any loss, actions, claims, proceedings, demand or costs or damages whatsoever or howsoever caused arising directly or indirectly in connection with or arising out of the use of this material.

## The molecular and crystal structure of 4-methoxybenzylidene-4'-*n*-butylaniline (MBBA) at $-163^{\circ}\text{C}$

by R. BOESE\*†, M. YU. ANTIPIN\*†‡,  
M. NUSSBAUMER† and D. BLÄSER†

† Institut für Anorganische Chemie der Universität-GH Essen,  
Universitätsstr. 5-7, 4300 Essen 1, Germany

‡ Institute of Organoelement Compounds, Russian Academy  
of Sciences, 117813 Moscow, Vavilov str., 28, Russia

(Received 9 October 1991; accepted 26 November 1991)

The molecular and crystal structure of the classic nematogen 4-methoxybenzylidene-4'-*n*-butylaniline (MBBA) was determined by X-ray diffraction method at  $-163^{\circ}\text{C}$  (diffractometer Nicolet R3m/V, Mo-radiation, 2256 observable reflections,  $R=0.058$ ). The monocrystal of MBBA was grown from the polycrystalline sample in a thin capillary at  $-163^{\circ}\text{C}$  by a new method using miniature zone melting procedure with a focused IR laser beam for producing a local molten zone. The crystals are orthorhombic:  $a=14.908(4)\text{Å}$ ,  $b=8.391(3)\text{Å}$ ,  $c=18.411(4)\text{Å}$ ,  $Z=6$ , space group  $P 2_1$ . Three independent molecules in the crystal have slightly different conformations but the geometric parameters are normal. The molecular packing is smectic-like and is characterized by the presence of layers parallel to (001), the thickness of the layer is close to the  $c$  axis of the unit cell. The relationship between the different phases of solid MBBA is discussed.

### 1. Introduction

4-Methoxybenzylidene-4'-*n*-butylaniline (MBBA) is a widely known thermotropic mesogenic material which is used in many aspects as a model compound for liquid crystal studies. It forms a nematic phase near room temperature between  $19$  and  $36^{\circ}\text{C}$  and in most handbooks on liquid crystals (see, for example, [1, 2]) it is cited as the simplest and classic representative of this kind of liquid crystal mesophase. The elongated molecule of MBBA contains a central 'rigid' fragment and a flexible alkyl chain on the periphery that is a necessary condition for the formation of this type of mesophase.

On cooling, MBBA forms a variety of solid state phases, including a glassy state (by fast cooling) and solid crystalline polymorphic modifications. The pattern of the phase transitions in solid MBBA is rather complicated: ten different phases of this compound (including nematic and isotropic) have been found by neutron diffraction, X-ray, DSC and Raman scattering methods [3-6]. Moreover, solid MBBA is characterized by the coexistence throughout the whole temperature interval of the solid state of at least two different modifications at one temperature; this was named in [3] as a multimode polymorphism. The known solid phases of MBBA are designated as  $C_0$  (glassy state),  $C_1$  and  $C_2$  (relaxed amorphous states),  $C_3$  and  $C_4$  (metastable crystalline states),  $C_5$  and  $C_6$  (stable crystalline phases) [5]. Nevertheless, no detailed structural information about the crystal symmetry, cell parameters, space group, molecular and crystal structure of MBBA for even one of these solid phases has been known until now, despite the

\* Authors for correspondence.

numerous attempts of growing monocrystals of this compound by crystallization from different solvents, directly from the melt or from the mesophase [7]. The low melting point and the very complicated nature of the polymorphism of MBBA, especially near this point, prevented the growth of monocrystals suitable for X-ray or neutron diffraction studies.

On the other hand, monocrystal structural data for solid precursors of the different liquid-crystalline phases are sometimes very important for understanding the essential features of the molecular organization in the mesophases, where usual diffraction methods alone cannot give unequivocal information about the mesophase structure.

It was shown earlier by a series of investigations (see, for example, the reviews [8, 9]) that some supramolecular fragments (molecular associates formed by strong intermolecular interaction) such as stacks and layers, which are often present in the crystal structures, may also be retained in the mesophases. If this general approach is to be taken into account, it is clear that direct information about the molecular and crystal structure of MBBA is of great interest. It is obvious, however, that the solution of this problem is related mainly with the development of some new crystallization methods of this low melting compound.

One of the well-known techniques for growing suitable monocrystals for X-ray data collection of low melting materials directly in the diffractometer is miniature zone melting crystallization with samples sealed in capillaries, flushed by a cold gas stream. Different methods for local heating and melting the samples in the thin walled capillaries have been used and applied for numerous structure determinations [10–12]. By far the most advantageous in many respects is the use of focused infrared light, from a halogen lamp [10]. However, high temperature gradients cannot be reached in all of these procedures. It was shown [13] that using an adjustable (control unit Type 05 LCM 350, Mellers–Giroto) CO<sub>2</sub> laser beam (20 W, Type 05 CRF 222-1, Mellers–Giroto) on an optical bench and focusing the beam with a ZnSe lens ( $f=127$  mm, diameter of the beam at the capillary approximately 0.2 mm) and a turnable mirror for controlling the focus position provides the possibility to obtain a very high temperature gradient and a very fine molten zone by local heating of the sample in the capillary. The scanning speed of the laser beam has to be adjusted to the crystallization speed of the sample under investigation and the beam intensity must be just sufficient to melt the material according to the temperature of the cold gas stream which is cooling the capillary. Intermediate phases between the liquid state and the phase to be investigated may be avoided, therefore, in this procedure which is essential to obtain monocrystals of the polymorphic modifications of different substances, including MBBA.

This technique for growing the MBBA monocrystal at  $-163^{\circ}\text{C}$  using a CO<sub>2</sub> laser beam for producing a molten zone within the polycrystalline material was applied and the crystal and molecular structure of the low temperature phase of this compound is presented here.

## 2. Experimental, structure solution and refinement

MBBA was placed in a 0.3 mm quartz capillary and cooled in a Nicolet R3m/V diffractometer (Mo-K<sub>α</sub> radiation, graphite monochromator) to  $-163^{\circ}\text{C}$ . A crystal was grown by means of a miniature zone melting procedure using a focused infrared laser beam [13]. Several scanning cycles of the molten zone along the capillary (speed 0.5 mm h<sup>-1</sup>, at a capillary length of 6 mm) purified the sample and simultaneously

provided a cylindrical monocrystal. The laser beam intensity was set to approximately 5 per cent of the maximum power (20 W).

The cell dimensions were determined from the diffractometer angles of 30 centred reflections ( $15^{\circ} \leq 2\Theta \leq 25^{\circ}$ ):  $a = 14.908(4) \text{ \AA}$ ,  $b = 8.391(3) \text{ \AA}$ ,  $c = 18.411(4) \text{ \AA}$ ,  $\beta = 96.40(2)^{\circ}$ ,  $V = 2288.7 \text{ \AA}^3$ ,  $Z = 6$ , monoclinic, spacegroup  $P 2_1$ ,  $\rho_{\text{calc}} = 1.169 \text{ g cm}^{-3}$ ,  $\mu = 0.06 \text{ mm}^{-1}$ . The intensities were measured with Wyckoff scan mode (scan range  $= 0.65^{\circ}$ ) for  $+h+k \pm l$  in the  $2\Theta$  range  $3^{\circ}$ – $50^{\circ}$ . With Lorentz and polarization corrections a volume correction for cylindrical crystals exceeding the diameter of the incident X-ray beam has been applied. The structure solution was performed by direct methods, atomic positions were refined in full matrix least squares using SHELXTL-Plus (Vers. 4.2/V). The refinement included anisotropic displacement parameters for non-hydrogen atoms and isotropic thermal parameters for hydrogen atoms, 540 parameters, 3000 unique intensities and 2256 observed ( $F_0 \geq 4\sigma(F_0)$ ),  $R = 0.0582$ ,  $R_w = 0.0568$ ,  $w^{-1} = \sigma^2(F_0) + 0.00081 * F_0^2$ , no extinction correction, maximum residual electron density  $0.289 \text{ e/\AA}^{-3}$ . The atomic coordinates are listed in table 1 bond lengths are given in table 2 and angles in table 3.

### 3. Results and discussion

#### 3.1. Molecular geometry and conformation

The unit cell of the low temperature phase of MBBA studied contains three independent molecules (figure 1), their conformations being different. In figure 2 all of the three independent molecules superimposed on the central  $-\text{C}-\text{C}=\text{N}-$  plane are shown schematically. This kind of so-called conformational polymorphism is quite usual for solid crystals structures of the precursors to the liquid-crystalline phase.

The geometry of the MBBA molecules is quite normal and close to that for other known 4,4'-disubstituted benzylideneaniline (BA) derivatives [7, 14–16]. The central BA fragment is essentially non-planar for the first (I) and second (II) independent molecules: dihedral angles  $\phi$  and  $\vartheta$  (see figure 3) are equal to  $3.9$  and  $24.1^{\circ}$  for I, and  $6.5$  and  $27.7^{\circ}$  for II, the inter-ring mean plane angle being  $27.7$  and  $29.6^{\circ}$ , respectively. In contrast to I and II the third independent molecule (III) the same BA fragment is almost planar:  $\phi = 2.5^{\circ}$ ,  $\vartheta = 2.2^{\circ}$ , the angle between ring planes is  $4.6^{\circ}$ . The torsion angles  $\tau(\text{C}-\text{C}=\text{N}-\text{C})$  are  $\tau(\text{I}) = -177.4^{\circ}$ ,  $\tau(\text{II}) = 176.0^{\circ}$  and  $\tau(\text{III}) = 178.9^{\circ}$ . According to *ab initio* calculations [17], the minimum energy of the BA molecule in the free state corresponds to dihedral angles  $\phi = 0^{\circ}$  and  $\vartheta = 45^{\circ}$ . Our data for MBBA and numerous X-ray structural data for its mesogenic fluorinated analogues [7, 14–16] show unequivocally that in the crystal state these two angles in BA derivatives are characterized by a large scatter ( $\phi = 0$ – $15^{\circ}$  and  $\vartheta = 2$ – $52^{\circ}$  [7]) which may be explained by the crystal field influence on the molecular conformation. As is known, more effective and energetically favourable crystal packing may result to the observed conformational changes [18].

The conformation and orientation of the terminal butyl groups is also different for molecules I–III. In molecules I and III these groups have an almost planar transoid conformation with torsion angles  $\text{C}(12)-\text{C}(15)-\text{C}(16)-\text{C}(17)$   $173.7^{\circ}$ ,  $\text{C}(15)-\text{C}(16)-\text{C}(17)-\text{C}(18)$   $-178.7^{\circ}$  in I and  $\text{C}(52)-\text{C}(55)-\text{C}(56)-\text{C}(57)$   $179.6^{\circ}$ ,  $\text{C}(55)-\text{C}(56)-\text{C}(57)-\text{C}(58)$   $173.7^{\circ}$  in III. All atoms of the butyl groups are coplanar within  $0.008$  and  $0.038 \text{ \AA}$  and dihedral angles between their planes and phenyl rings planes are equal to  $67.0$  and  $77.3^{\circ}$ . In molecule II torsion angles  $\text{C}(32)-\text{C}(35)-\text{C}(36)-\text{C}(37)$   $-177.1^{\circ}$  and  $\text{C}(35)-\text{C}(36)-\text{C}(37)-\text{C}(38)$   $-68.6^{\circ}$  correspond to a nearly *gauche* conformation of the side chain. Atoms  $\text{C}(32)$ ,  $\text{C}(35)$ ,  $\text{C}(36)$ ,  $\text{C}(37)$  are coplanar within  $0.018 \text{ \AA}$  and  $\text{C}(38)$  deviates from this plane by

Table 1. Atomic coordinates and equivalent isotropic displacement factors of MBBA.

	$x/10^{-4}$	$y/10^{-4}$	$z/10^{-4}$	$U_{eq}/10^{-1} \text{ pm}^2 \dagger$
C(1)	3614(5)	693	7598(4)	349(30)
C(2)	4306(5)	1422(16)	7297(3)	359(29)
C(3)	4335(4)	1477(15)	6555(3)	262(26)
C(4)	3648(4)	745(15)	6092(3)	276(27)
C(5)	2941(5)	-11(15)	6397(4)	335(28)
C(6)	2925(4)	-12(15)	7145(3)	335(28)
C(7)	3686(4)	668(15)	5293(3)	255(26)
C(8)	4397(4)	1116(15)	4246(4)	250(27)
C(9)	4876(4)	2281(15)	3921(3)	318(28)
C(10)	5007(5)	2175(16)	3177(4)	328(29)
C(11)	4656(4)	925(16)	2756(3)	275(28)
C(12)	4179(5)	-237(15)	3097(4)	335(29)
C(13)	4052(5)	-148(15)	3829(3)	302(28)
C(14)	4772(5)	828(16)	1943(3)	396(31)
C(15)	3980(5)	1471(19)	1475(4)	686(42)
C(16)	4039(6)	1327(19)	648(4)	781(45)
C(17)	4762(6)	2402(21)	387(5)	934(55)
C(18)	2972(6)	-86(18)	8670(4)	574(38)
C(19)	7375(4)	1427(15)	6169(3)	282(27)
C(20)	8050(4)	2082(15)	5779(3)	299(28)
C(21)	7989(4)	1753(15)	5027(3)	293(28)
C(22)	7297(4)	876(15)	4678(3)	276(27)
C(23)	6625(4)	250(15)	5083(4)	310(27)
C(24)	6673(4)	517(15)	5827(3)	296(28)
C(25)	7228(5)	527(15)	3880(3)	274(27)
C(26)	7757(4)	765(14)	2740(3)	255(26)
C(27)	8414(4)	1494(16)	2362(3)	321(28)
C(28)	8431(5)	1201(16)	1630(3)	331(28)
C(29)	7825(5)	211(16)	1230(3)	312(27)
C(30)	7152(5)	-491(16)	1609(4)	380(30)
C(31)	7116(5)	-214(16)	2347(4)	379(31)
C(32)	7854(5)	-105(16)	431(3)	410(31)
C(33)	7177(4)	891(15)	-62(3)	361(29)
C(34)	7210(4)	548(16)	-875(3)	353(29)
C(35)	6473(5)	1398(17)	-1357(3)	497(33)
C(36)	8038(5)	2621(15)	7279(3)	387(31)
C(37)	1240(4)	1456(15)	3578(3)	256(26)
C(38)	1708(5)	2219(15)	4190(3)	278(27)
C(39)	1398(4)	1952(16)	4866(3)	316(29)
C(40)	647(4)	1036(15)	4946(3)	245(25)
C(41)	194(4)	305(15)	4322(3)	263(27)
C(42)	488(4)	550(15)	3643(3)	275(26)
C(43)	346(4)	764(15)	5668(3)	312(28)
C(44)	481(4)	1132(15)	6940(3)	238(26)
C(45)	728(4)	2266(15)	7465(3)	289(27)
C(46)	513(5)	2060(16)	8175(3)	314(29)
C(47)	92(4)	700(15)	8376(3)	264(27)
C(48)	-138(5)	-466(15)	7859(4)	298(27)
C(49)	61(4)	-250(16)	7133(3)	296(28)
C(50)	-100(5)	477(16)	9168(3)	350(29)
C(51)	767(4)	350(16)	9697(3)	371(28)
C(52)	569(5)	311(17)	10500(3)	443(31)
C(53)	1415(5)	225(17)	11017(4)	594(38)
C(54)	2222(5)	2647(16)	2786(4)	428(33)

Table 1 (continued).

	$x/10^{-4}$	$y/10^{-4}$	$z/10^{-4}$	$U_{\text{eq}}/10^{-1} \text{ pm}^2 \dagger$
O(1)	3675(3)	688(13)	8348(2)	394(20)
O(2)	7347(3)	1662(13)	6905(2)	293(18)
O(3)	1479(3)	1636(13)	2882(2)	343(19)
N(1)	4348(4)	1296(14)	5006(3)	270(22)
N(2)	7813(4)	1119(14)	3497(3)	357(25)
N(3)	749(3)	1446(14)	6230(3)	274(22)

† Equivalent isotropic  $U$  calculated as one third of the trace of the orthogonalized  $U_{ij}$  tensor.

Table 2. Bond distance ( $\text{\AA}$ ) in MBBA.

C(1)–C(2)	1.368 (11)	C(1)–C(6)	1.381 (10)
C(1)–O(1)	1.373 (8)	C(2)–C(3)	1.372 (9)
C(3)–C(4)	1.400 (11)	C(4)–C(5)	1.400 (12)
C(4)–C(7)	1.479 (9)	C(5)–C(6)	1.381 (9)
C(7)–N(1)	1.284 (10)	C(8)–C(9)	1.385 (14)
C(8)–C(13)	1.375 (15)	C(8)–N(1)	1.417 (8)
C(9)–C(10)	1.409 (10)	C(10)–C(11)	1.373 (15)
C(11)–C(12)	1.397 (14)	C(11)–C(14)	1.528 (9)
C(12)–C(13)	1.383 (10)	C(14)–C(15)	1.483 (12)
C(15)–C(16)	1.539 (10)	C(16)–C(17)	1.524 (18)
C(18)–O(1)	1.419 (12)	C(19)–C(20)	1.411 (11)
C(19)–C(24)	1.388 (12)	C(19)–O(2)	1.376 (8)
C(20)–C(21)	1.404 (9)	C(21)–C(22)	1.367 (12)
C(22)–C(23)	1.413 (11)	C(22)–C(25)	1.492 (9)
C(23)–C(24)	1.382 (9)	C(25)–N(2)	1.281 (11)
C(26)–C(27)	1.402 (12)	C(26)–C(31)	1.399 (13)
C(26)–N(2)	1.420 (9)	C(27)–C(28)	1.374 (9)
C(28)–C(29)	1.378 (13)	C(29)–C(30)	1.413 (12)
C(29)–C(32)	1.499 (9)	C(30)–C(31)	1.386 (10)
C(32)–C(33)	1.529 (12)	C(33)–C(34)	1.531 (9)
C(34)–C(35)	1.512 (12)	C(36)–O(2)	1.423 (11)
C(37)–C(38)	1.410 (11)	C(37)–C(42)	1.371 (12)
C(37)–O(3)	1.376 (8)	C(38)–C(39)	1.393 (10)
C(39)–C(40)	1.379 (13)	C(40)–C(41)	1.408 (11)
C(40)–C(43)	1.467 (9)	C(41)–C(42)	1.385 (9)
C(43)–N(3)	1.272 (10)	C(44)–C(45)	1.377 (14)
C(44)–C(49)	1.382 (16)	C(44)–N(3)	1.434 (9)
C(45)–C(46)	1.392 (10)	C(46)–C(47)	1.372 (16)
C(47)–C(48)	1.382 (14)	C(47)–C(50)	1.528 (9)
C(48)–C(49)	1.413 (10)	C(50)–C(51)	1.532 (9)
C(51)–C(52)	1.540 (9)	C(52)–C(53)	1.496 (10)
C(54)–O(3)	1.421 (12)		

Table 3. Bond angles (°) in MBBA.

C(2)–C(1)–C(6)	119.3(6)	C(2)–C(1)–O(1)	116.1(6)
C(6)–C(1)–O(1)	124.5(6)	C(1)–C(2)–C(3)	121.9(7)
C(2)–C(3)–C(4)	119.2(7)	C(3)–C(4)–C(5)	119.2(6)
C(3)–C(4)–C(7)	121.2(7)	C(5)–C(4)–C(7)	119.6(7)
C(4)–C(5)–C(6)	119.9(7)	C(1)–C(6)–C(5)	120.5(7)
C(4)–C(7)–N(1)	120.5(7)	C(9)–C(8)–C(13)	118.8(7)
C(9)–C(8)–N(1)	115.9(9)	C(13)–C(8)–N(1)	125.2(9)
C(8)–C(9)–C(10)	120.7(10)	C(9)–C(10)–C(11)	120.8(10)
C(10)–C(11)–C(12)	117.4(7)	C(10)–C(11)–C(14)	121.1(9)
C(12)–C(11)–C(14)	121.5(9)	C(11)–C(12)–C(13)	122.2(10)
C(8)–C(13)–C(12)	120.2(10)	C(11)–C(14)–C(15)	112.4(7)
C(14)–C(15)–C(16)	114.6(8)	C(15)–C(16)–C(17)	112.7(9)
C(20)–C(19)–C(24)	121.8(6)	C(20)–C(19)–O(2)	123.2(8)
C(24)–C(19)–O(2)	115.0(7)	C(19)–C(20)–C(21)	117.0(8)
C(20)–C(21)–C(22)	122.0(7)	C(21)–C(22)–C(23)	119.6(6)
C(21)–C(22)–C(25)	122.3(7)	C(23)–C(22)–C(25)	118.1(7)
C(22)–C(23)–C(24)	120.0(8)	C(19)–C(24)–C(23)	119.5(7)
C(22)–C(25)–N(2)	119.3(8)	C(27)–C(26)–C(31)	118.4(6)
C(27)–C(26)–N(2)	115.4(8)	C(31)–C(26)–N(2)	126.3(7)
C(26)–C(27)–C(28)	119.9(8)	C(27)–C(28)–C(29)	123.4(8)
C(28)–C(29)–C(30)	116.5(6)	C(28)–C(29)–C(32)	122.8(8)
C(30)–C(29)–C(32)	120.8(8)	C(29)–C(30)–C(31)	121.5(9)
C(26)–C(31)–C(30)	120.4(8)	C(29)–C(32)–C(33)	113.3(8)
C(32)–C(33)–C(34)	112.8(8)	C(33)–C(34)–C(35)	112.6(7)
C(38)–C(37)–C(42)	121.2(6)	C(38)–C(37)–O(3)	122.5(8)
C(42)–C(37)–O(3)	116.2(7)	C(37)–C(38)–C(39)	117.2(8)
C(38)–C(39)–C(40)	122.6(7)	C(39)–C(40)–C(41)	118.5(6)
C(39)–C(40)–C(43)	121.2(7)	C(41)–C(40)–C(43)	120.3(8)
C(40)–C(41)–C(42)	120.0(8)	C(37)–C(42)–C(41)	120.3(7)
C(40)–C(43)–N(3)	120.1(8)	C(45)–C(44)–C(49)	119.5(7)
C(45)–C(44)–N(3)	115.6(9)	C(49)–C(44)–N(3)	124.7(9)
C(44)–C(45)–C(46)	120.1(10)	C(45)–C(46)–C(47)	121.1(9)
C(46)–C(47)–C(48)	119.3(7)	C(46)–C(47)–C(50)	119.9(9)
C(48)–C(47)–C(50)	120.8(10)	C(47)–C(48)–C(49)	119.9(10)
C(44)–C(49)–C(48)	120.0(9)	C(47)–C(50)–C(51)	112.3(5)
C(50)–C(51)–C(52)	112.0(5)	C(51)–C(52)–C(53)	112.0(6)
C(1)–O(1)–C(18)	116.9(6)	C(19)–O(2)–C(36)	117.3(6)
C(37)–O(3)–C(54)	117.8(6)	C(7)–N(1)–C(8)	119.3(7)
C(25)–N(2)–C(26)	119.4(8)	C(43)–N(3)–C(44)	120.3(8)

1.27 Å. The dihedral angle between the mean plane butyl group (four C atoms are coplanar only within 0.229 Å) and ring plane is equal to 54.7°. Nevertheless, despite the different conformation, all three independent MBBA molecules have nearly the same length in the crystal, the intramolecular distances C(1)...C(18), C(21)...C(38) and C(41)...C(58) are 15.47, 15.91 and 15.85 Å. It should be noted that none of these molecules has the extremely elongated possible length because the flexible alkyl chains are inclined to the nearest ring planes and thereby MBBA molecules have a slightly curved shape.

### 3.2. The molecular packing

Crystal packing projections of the MBBA structure are shown in figures 4 and 5. The long axis of all molecules in the crystal are oriented in the same direction (nearly along the *c* axis). This parallel packing mode is quite usual for the solid crystal state of

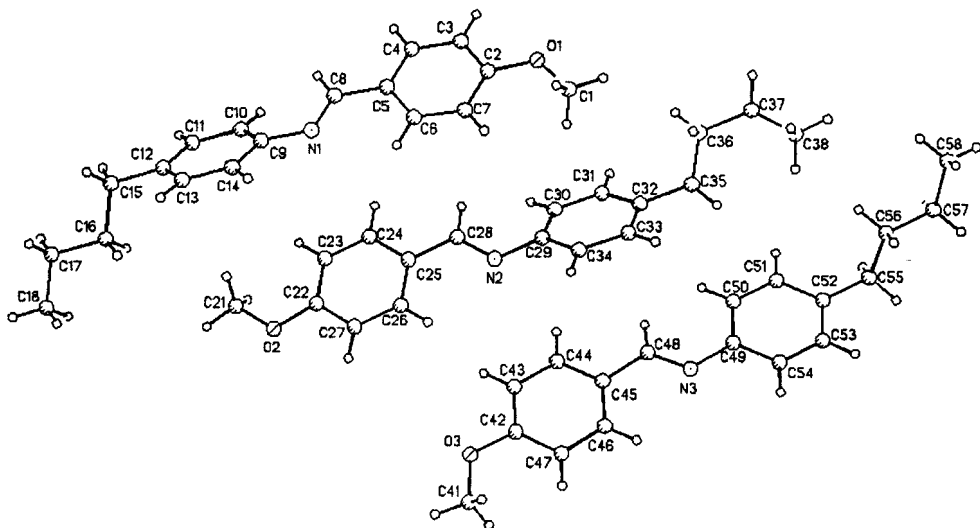


Figure 1. The molecular structure of MBBA with the numbering scheme of the three independent molecules.

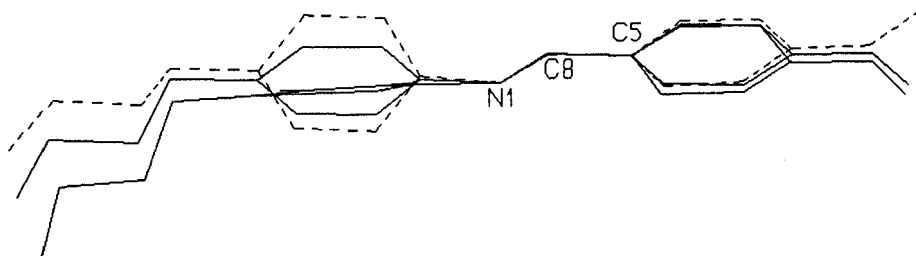


Figure 2. Superimposition of the three independent molecules of MBBA.

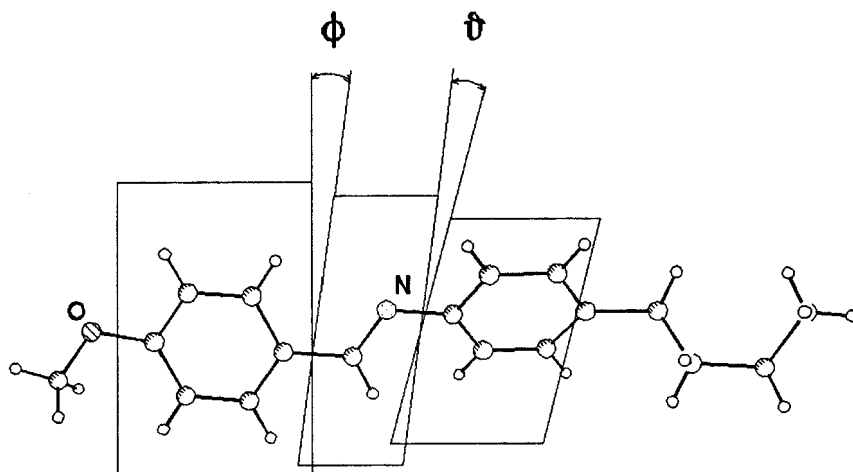


Figure 3. The definition of the interplanar angles in the BA moiety of MBBA.



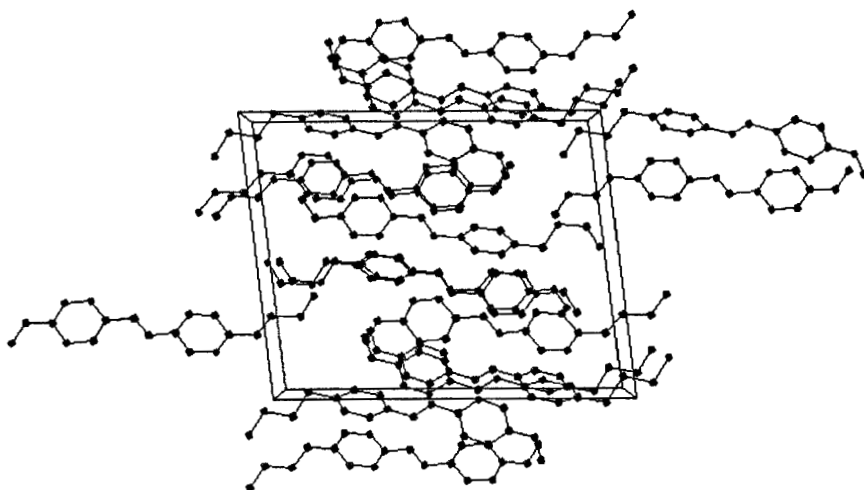


Figure 4. Molecular packing of MBBA in the 010 direction.

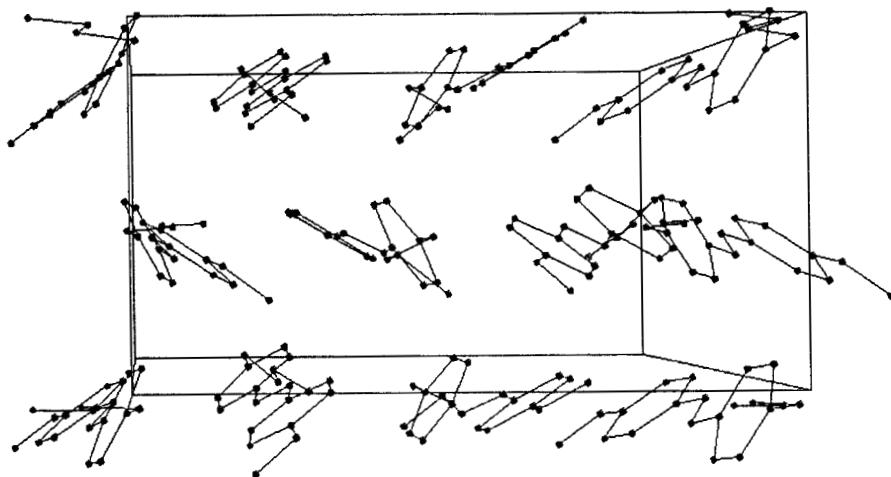


Figure 5. Molecular packing of MBBA in the 001 direction.

the nematic precursors. The long axis of the independent molecules I and III are antiparallel, but molecule II is oriented nearly parallel to I. Nevertheless, the crystal packing type in MBBA, found in this work, differs essentially from that typically found for nematics.

The more important feature of the packing motive in the MBBA phase studied is that the molecules are associated in layers parallel to (001), which are clearly seen in figures 4 and 5. Each molecule in the layer is surrounded by six neighbours and its orientation is nearly normal to the mean plane of the layer. The thickness of the layer is close to the  $c$  axis of the unit cell (18.41 Å) and comparable with the molecular length ( $\sim 19$  Å). There is no essential mutual penetration of molecules into the adjacent layers which would be very typical for nematic structures [8, 9]. Namely this penetration in nematic precursors results in the characteristic imbrication-type of packing in their crystals. It should be noted, however, that these layers in the crystal structure of MBBA

are not similar to the layers in the smectic-like relaxed amorphous states  $C_1$  and  $C_2$ , found earlier in these phases of MBBA by the low angle neutron diffraction method [6]. For these two non-equilibrium phases, which may be obtained by fast cooling of the liquid-crystalline phase, a bilayer type of the molecular packing was assumed with the layer thickness of *c.* 32.8 and 33.4 Å.

Not a single analogue of the MBBA crystal structure was found among the large series of its mesomorphous fluorinated derivatives [14–16]. The closest analogue to the MBBA structure was found to be the crystal structure of fluorinated 4-ethoxybenzylidene-4'-(4"-trifluorobutyl)aniline [19]. In the triclinic crystal of this compound (unit cell parameters are nearly of the same order of that for MBBA,  $a = 11.198$  Å,  $b = 14.592$  Å,  $c = 17.088$  Å,  $\alpha = 90.55^{\circ}$ ,  $\beta = 101.48^{\circ}$ ,  $\gamma = 102.49^{\circ}$ ), the three independent molecules also form layers but have dissimilar conformations.

Due to the previous difficulties of obtaining unequivocal, direct structural information about the packing modes of MBBA molecules in different phases some attempts were made to model this packing using atom–atom potential energy calculations [7, 20]. Such a computational approach was found to be very useful in the liquid crystal mesophase structure studies. The theoretically calculated crystal structure found for MBBA [7, 20] differs essentially from that found in this work. It should be noted, however, that in these calculations only models with one independent molecule were considered. Nevertheless, the important result of these calculations is that two energetically preferable structures of MBBA were found, one structure with the nematic-like parallel molecular organization and the second one with the layered type of packing. The unit cell parameters of these hypothetical structures ( $a = 8.21$  Å,  $b = 5.41$  Å,  $c = 36.39$  Å,  $\beta = 96.9^{\circ}$ , space group  $P 2_1/c$  for the first one and  $a = 5.79$  Å,  $b = 7.44$  Å,  $c = 36.28$  Å, space group  $P 2_12_12_1$  for the second layered structure) differ from that found in the present work. Some variants of the monoclinic unit cell of MBBA for the  $C_5$  and  $C_6$  phases were also suggested in [5] on the basis of the experimental diffraction data, but these results were much closer to the calculations [7], than to our data.

We suspect that the modification which we have found in this work probably is the stable  $C_5$  modification of the solid MBBA, which is known to be thermodynamically stable below  $-68^{\circ}\text{C}$  [5]. The stable  $C_6$  modification may probably result from  $C_5$  by conformational motions of the flexible side chains. The method for low temperature monocrystal growing described, using a laser beam for the local heating of the sample, with a precisely controlled gas stream temperature may allow us to obtain information about other MBBA phases.

This work was supported by the Fonds der Chemischen Industrie, M.A. gratefully acknowledges a fellowship from the Heinrich–Hertz Stiftung.

### References

- [1] SHANDRASEKHAR, S., 1977, *Liquid Crystals* (Cambridge University Press), p. 342.
- [2] DE JEU, W. H., 1980, *Physical Properties of Liquid Crystalline Materials* (Gordon & Breach), p. 133.
- [3] DOLGANOV, V. K., KROÓ, N., ROSTA, L., SHEKA, E. F., and SZABON, J., 1985, *Molec. Crystals liq. Crystals*, **127**, 187.
- [4] ROSTA, L., KROÓ, N., TÖRÖK, GY., and PÉPY, G., 1987, *Molec. Crystals liq. Crystals*, **146**, 403.
- [5] ROSTA, L., KROÓ, N., DOLGANOV, V. K., PACHER, P., SIMKIN, V. G., TÖRÖK, GY., and PÉPY, G., 1987, *Molec. Crystals liq. Crystals*, **144**, 297.

- [6] PÉPY, G., FOURET, R., MORE, M., and ROSTA, L., 1989, *Physica scripta*, **39**, 485.
- [7] SEREDA, S. V., TIMOFEEVA, T. V., ANTIPIN, M. YU., and STRUCHKOV, YU. T., 1992, *Liq. Crystals*, **11**, 839.
- [8] BRYAN, R. F., 1978, *Proceedings of the Pre-conference Symposium on Organic Crystal Chemistry*, Poznan, edited by Z. Kałuski (Adam Mickiewicz University Press), p. 106.
- [9] BRYAN, R. F., 1982, *Zh. strukt. Khim.* (U.S.S.R.), **23**, 154.
- [10] BRODALLA, D., MOOTZ, D., BOESE, R., and OSSWALD, W., 1985, *J. appl. Crystallogr.*, **18**, 316.
- [11] KRAVERS, M. A., ANTIPIN, M. YU., KULISHOV, V. I., and STRUCHKOV, YU. T., 1977, *Sov. Phys. Crystallogr. (Russian)*, **22**, 1118.
- [12] VEITH, M., and FRANK, W., 1988, *Chem. Rev.*, **88**, 81.
- [13] BOESE, R., BLÄSER, D., and NUSSBAUMER, M. (to be published).
- [14] SEREDA, S. V., ANTIPIN, M. YU., TIMOFEEVA, T. V., STRUCHKOV, YU. T., and SHELJAGENKO, S. V., 1987, *Sov. Phys. Crystallogr. (Russian)*, **32**, 352.
- [15] SEREDA, S. V., ANTIPIN, M. YU., TIMOFEEVA, T. V., STRUCHKOV, YU. T., and SHELJAGENKO, S. V., 1987, *Sov. Phys. Crystallogr. (Russian)*, **32**, 685.
- [16] SEREDA, S. V., ANTIPIN, M. YU., TIMOFEEVA, T. V., and STRUCHKOV, YU. T., 1988, *Sov. Phys. Crystallogr. (Russian)*, **33**, 845.
- [17] BERNSTEIN, J., ENGEL, J. M., and HAGLER, A. T., 1981, *J. chem. Phys.*, **75**, 2346.
- [18] BERNSTEIN, J., and IZEK, I., 1976, *J. chem. Soc. Perkin II*, 429.
- [19] SEREDA, S. V., ANTIPIN, M. YU., TIMOFEEVA, T. V., STRUCHKOV, YU. T., SHELJAGENKO, S. V., and FIALKOV, YU. A., 1989, *Soc. Phys. Crystallogr. (Russian)*, **34**, 333.
- [20] SEREDA, S. V., TIMOFEEVA, T. V., and STRUCHKOV, YU. T., 1991, *Sov. Phys. Crystallogr. (Russian)*, **36**, 446.